

ADVANCED MATERIALS

Supporting Information

for *Adv. Mater.*, DOI: 10.1002/adma.201501752

Self-Passivation of Defects: Effects of High-Energy Particle
Irradiation on the Elastic Modulus of Multilayer Graphene

*Kai Liu, Cheng-Lun Hsin, Deyi Fu, Joonki Suh, Sefaattin
Tongay, Michelle Chen, Yinghui Sun, Aiming Yan, Joonsuk
Park, Kin M. Yu, Wenli Guo, Alex Zettl, Haimei Zheng, Daryl
C. Chrzan, and Junqiao Wu**

Supporting Information

Self-passivation of defects: effects of high-energy particle irradiation on elastic modulus of multilayer graphene

*Kai Liu, Cheng-Lun Hsin, Deyi Fu, Joonki Suh, Sefaattin Tongay, Michelle Chen, Yinghui Sun, Aiming Yan, Joonsuk Park, Kin M. Yu, Wenli Guo, Alex Zettl, Haimei Zheng, Daryl C. Chrzan, and Junqiao Wu**

1. AFM topography of pristine bilayer and pentalayer graphene membranes

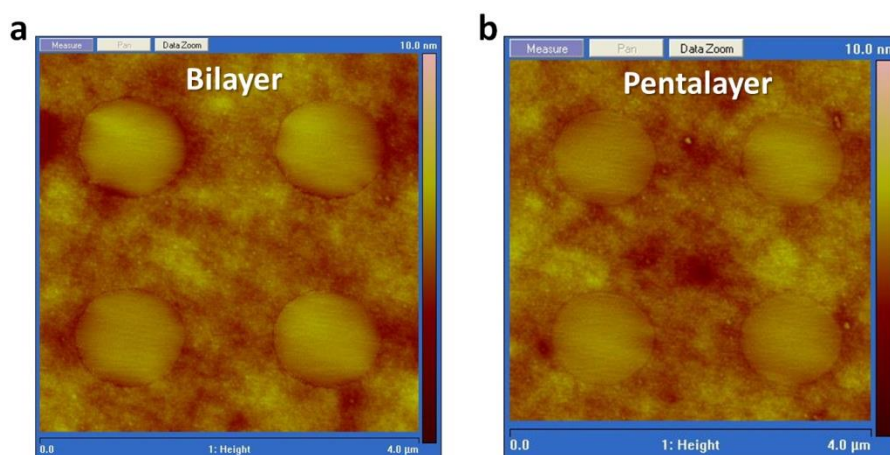


Figure S1. Taut, free-standing membranes of (a) bilayer and (b) pentalayer graphene.

2. AFM topography of pristine and irradiated graphene

An amorphous coating layer on the graphene appears after irradiation, especially at high irradiation doses (Figures S2 and S3). The coating layer is probably a thin layer of amorphous carbon contamination coming from residual gas or carbonaceous adsorbates. Such carbon contamination of materials is well known when the materials are bombarded with high energy particles even in high vacuum, such as sample characterization in electron microscopes. A recent study showed that even gently annealing exfoliated graphene at relatively low temperatures (~ 400 °C) causes amorphous carbon coating.^[S1] As revealed by AFM images

(Figure S2), when the cumulative irradiation dose is higher than $\sim 10^{13}$ ions cm^{-2} , a noticeable amorphous carbon layer starts to develop on the graphene. The amorphous carbon deposit is particles-like, especially at low or medium doses of irradiation (Figure S2b), and the deposit tends to become continuous at high doses (Figure S3a). Under a dose of 10^{15} ions cm^{-2} , the amorphous carbon thickness is ~ 1 nm (Figure S3a). The reported Young's modulus of amorphous carbon varies widely from <100 to >500 GPa,^[S2] and it is not dramatically lower than that of graphene (~ 1 TPa). As a result, these nm-scale particles deposits, even without in-plane connectivity, may enhance the in-plane stiffness of graphene, because they are still much larger than the C-C bond length (0.142 nm), such that each particle covers a large number of C-C bonds. These C-C bonds may appear to be pinned onto the amorphous particles when the graphene membrane is stretched, leading to a higher effective stiffness that depends on the coverage of amorphous carbon particles. Indeed, in our experiments we observe that the measured modulus of monolayer graphene was 333 N/m after the initial AFM scanning at a high irradiation dose (10^{15} ions/ cm^2), and the modulus stabilizes at 304 N/m after several cycles of scanning. Therefore, in order to minimize the influence of the amorphous carbon coating, we utilized the contact mode to scan the AFM tip over the graphene membrane to sweep away the amorphous carbon layer. The contact force is set to be small (~ 100 nN) to avoid damages to the graphene. It is shown in Figure S3 that the irradiated membrane becomes much cleaner and it keeps taut over the hole after the AFM sweeping, indicating that the sweeping does not generate ripples on the membrane. The Raman spectrum after the sweeping does not show any changes in the *D* peak, suggesting that the sweeping does not introduce any additional defects in the graphene membranes (Figure S4). Indentation as well as Raman measurements were then carried out on the AFM-cleaned graphene membranes under various doses of irradiation.

Here we note that we applied a small force during the AFM sweeping, but this force would induce different indentation depth for graphene samples with different number of layers, leading to different sweeping configurations. At high doses of irradiation, therefore, the amount of remaining deposit after the AFM sweeping is probably different for monolayer, bilayer, and pentalayer graphene, which makes it impossible to compare the increase in E^{2D} for these different samples in the range of high irradiation dose.

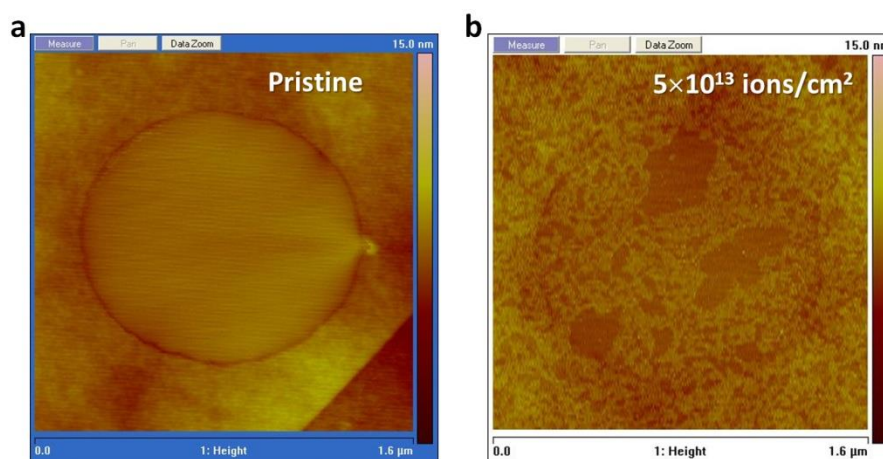


Figure S2. Comparison of (a) a pristine monolayer membrane, and (b) one after a medium-dose irradiation. The roughness in Figure b is caused by a thin, amorphous coating layer.

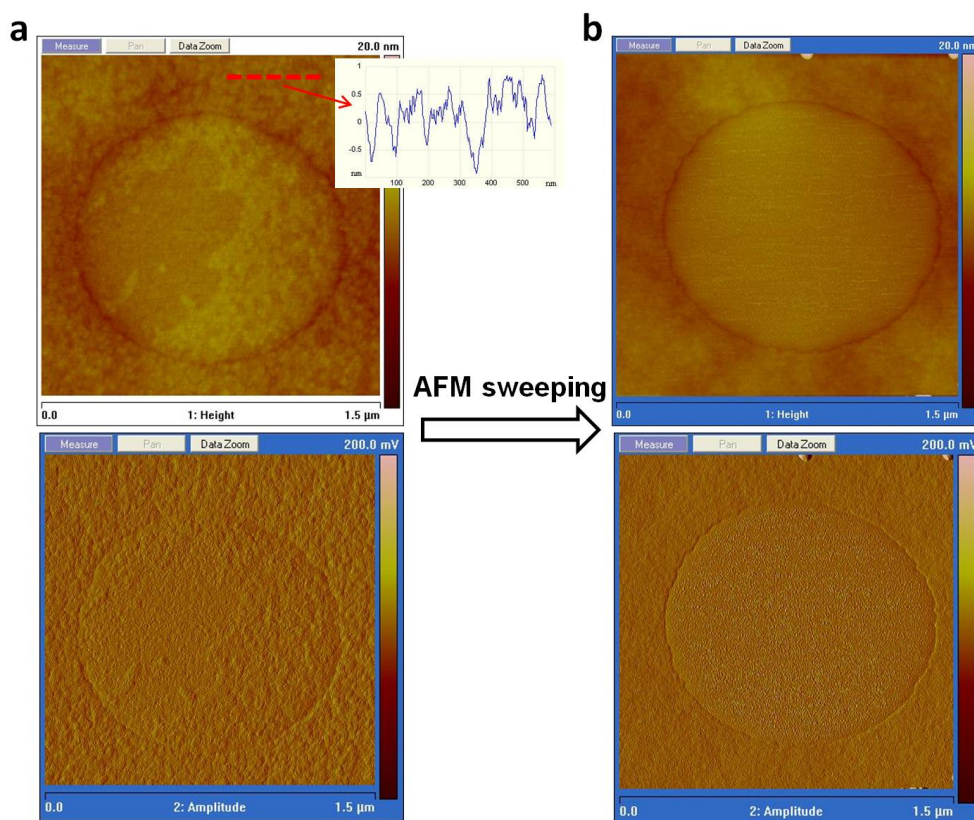


Figure S3. Comparison of (a) monolayer membrane as-irradiated at a dose of 1×10^{15} ions cm^{-2} and (b) the same membrane after the AFM contact-mode sweeping. The top images are height and the bottom ones are amplitude. A linear height scan of the as-irradiated sample on the substrate part (red dashed line) shows a surface roughness of ~ 1 nm. It can be seen that after the contact sweeping, the graphene surface is much cleaner because most of the amorphous carbon is swept away, but it still shows some tiny bumps which are the left coating residues.

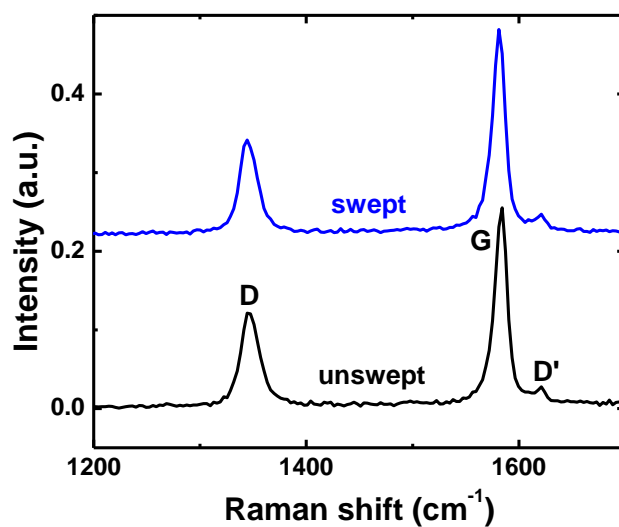


Figure S4. Comparison of Raman spectra before and after the AFM sweeping. The sample was irradiated by 3 MeV He²⁺ under a dose of 1×10^{15} ions cm⁻².

3. Pretensions at various doses for different layers of graphene

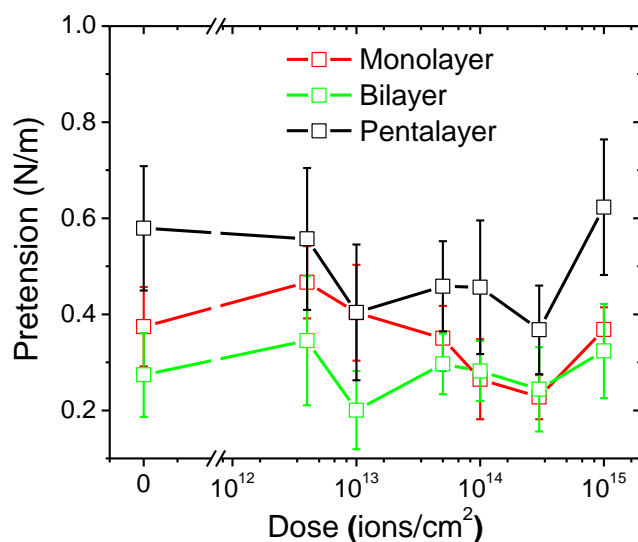


Figure S5. Pretensions at various doses for monolayer, bilayer, and pentalayer graphene.

References:

[S1] J. Hong, M. K. Park, E. J. Lee, D. Lee, D. S. Hwang, S. Ryu, *Sci. Rep.* **2013**, *3*, 2700.

[S2] B. Schultrich, H.-J. Scheibe, G. Grandremy, D. Schneider, *Phys. Stat. Sol. (a)* **1994**, *145*, 385.